Available online at www.sciencedirect.com
ScienceDirect
Applied Geochemistry 23 (2008) 408–418
Applied Geochemistry
www.elsevier.com/locate/apgeochem

Total particulate and reactive gaseous mercury in ambient air on the eastern slope of the Mt. Gongga area, China

Xuewu Fu [a,b], Xinbin Feng [a,*], Wanze Zhu [c], Wei Zheng [a,b], Shaofeng Wang [a,b], Julia Y. Lu [d]

[a] State Key Laboratory of Environmental Geochemistry, Institute of Geochemistry, Chinese Academy of Sciences, Guiyang 550002, PR China
[b] Graduate University of the Chinese Academy Sciences, Beijing 100049, PR China
[c] Institute of Mountain Hazards and Environment, Chinese Academy of Sciences, Chengdu 610041, PR China
[d] Department of Chemistry and Biology, Ryerson University, Toronto, Ont., Canada M5B 2K3

Available online 1 January 2008

Abstract

Total particulate mercury (TPM) and reactive gaseous mercury (RGM) concentrations in ambient air on the eastern slope of the Mt. Gongga area, Sichuan Province, Southwestern China were monitored from 25 May, 2005 to 29 April, 2006. Simultaneously, Hg concentrations in rain samples were measured from January to December, 2006. The average TPM and RGM concentrations in the study site were 30.7 and 6.2 pg m^{-3}, which are comparable to values observed in remote areas in Northern America and Europe, but much lower than those reported in some urban areas in China. The mean seasonal RGM concentration was slightly higher in spring (8.0 pg m^{-3}) while the minimum mean concentration was observed in winter (4.0 pg m^{-3}). TPM concentrations ranged across two orders of magnitude from 5.2 to 135.7 pg m^{-3} and had a clear seasonal variation: winter (74.1 pg m^{-3}), autumn (22.5 pg m^{-3}), spring (15.3 pg m^{-3}) and summer (10.8 pg m^{-3}), listed in decreasing order. The annual wet deposition was 9.1 μg m^{-2} and wet deposition in the rainy season (May–October) represented over 80% of the annual total. The temporal distribution of TPM and RGM suggested distinguishable dispersion characteristics of these Hg species on a regional scale. Elevated TPM concentration in winter was probably due to regional and local enhanced coal burning and low wet deposition velocity. The RGM distribution pattern is closely related to daily variation in UV radiation observed during the winter sampling period indicating that photo-oxidation processes and diurnal changes in meteorology play an important role in RGM generation.

1. Introduction

Mercury is a highly toxic environmental pollutant that can cause great harm to the environment and human health (Schroeder and Munthe, 1998). Since the industrial revolution, Hg released from human activities has significantly increased and it has been estimated that the average Hg concentration in the troposphere has increased by a factor of 3 (Fitzgerald, 1995). Due to its volatility, Hg can be transported over a long distance via the atmosphere to remote areas once emitted from sources. Elevated Hg concentrations in the air can cause contamination of remote areas via

* Corresponding author. Fax: +86 851 5891609.
E-mail address: fengxinbin@vip.skleg.cn (X. Feng).

0883-2927/$ - see front matter © 2007 Elsevier Ltd. All rights reserved.
doi:10.1016/j.apgeochem.2007.12.018

atmospheric transport followed by wet and dry deposition (Miller et al., 2005). Studies of Hg pollution in lake sediments, peat bogs and glacier ice have illuminated the increased contamination in remote areas after industrialization (Lorey and Driscoll, 1999; Schuster et al., 2002; Yang and Rose, 2003).

Once released from point sources, Hg speciation determinates its fate and transport in the atmosphere (Lindberg and Stratton, 1998). Generally, atmospheric Hg consists of three different chemical and physical forms including gaseous elemental mercury (GEM or Hg^0), divalent reactive gaseous mercury (RGM), and particulate bound mercury (TPM) (Lindberg and Stratton, 1998). RGM (e.g., $HgCl_2$, $HgOH_2$ and $HgBr_2$) and TPM are the significant fractions of Hg emissions from municipal waste incinerations and coal-fired power plants (Prestbo and Bloom, 1995). Recent studies have suggested that RGM emitted from anthropogenic sources can represent more than 30% of total Hg released (Pacyna et al., 2003; Streets et al., 2005; Wu et al., 2006). RGM is highly water-soluble (at least 5 orders magnitude higher than Hg^0) and has an extremely high dry deposition velocity (0.4–5.9 cm/s, Lindberg and Stratton, 1998). These characteristics cause RGM concentrations to decrease rapidly with distance from their primary sources and RGM is not considered an air pollutant that is transported long distances (Landis et al., 2004). Generally, RGM concentrations in remote areas are documented in the range from below detection limits to several hundreds of pg m^{-3} and can represent 1–3% of total gaseous mercury (TGM) in the air (Landis et al., 2002; Poissant et al., 2004). However, several events in which RGM comprised over 60% of the TGM in air have been observed (e.g., Barrow, Alaska; Lindberg et al., 2001). A significantly high RGM concentration of 100 ng m^{-3} was also observed in a Hg smelting workshop in Guizhou Province in SW China (Tan et al., 2000). TPM consists of Hg (Hg^0 and RGM) bound or adsorbed to atmospheric particles including dust, soot, sea-salt aerosols, etc. It is present in the atmosphere at low pg m^{-3} levels and generally represents less than 10% of total Hg in the air (Lu and Schroeder, 2004). Particulate Hg is not the major form emitted directly to the atmosphere (Pacyna et al., 2003). However, very fast transfer from RGM to TPM and oxidation of Hg^0 during transport of air masses would contribute an increased concentration of TPM and depletion of RGM in the atmosphere (Poissant et al., 2005; Lynam and Keeler, 2005). Compared to RGM, dry deposition velocities for TPM (0.1–2.1 cm/s, Lindberg and Stratton, 1998; Poissant et al., 2004) are lower and depended on particle size (Zhang et al., 2001). A modeling study (Lee et al., 2001) suggests that TPM is deposited predominantly in wet deposition, in contrast to RGM which is predominantly attributable to dry deposition.

Even though present as a small proportion of total Hg in the atmosphere, TPM and RGM have been suggested to be crucial in Hg transport and removal processes (Lindberg and Stratton, 1998). Hg^0 is a stable form of Hg, which has much lower water solubility and is commonly not considered in the wet deposition of Hg (Lee et al., 2001; Seigneur et al., 2003). Moreover, dry deposition of Hg^0 is lower by at least 1–2 orders of magnitude than TPM and RGM. Thus, even trace amounts of RGM and TPM species may contribute predominantly to the deposition of Hg (Lindberg and Stratton, 1998; Lee et al., 2001). In recent years, more and more studies have considered the concentrations and chemical speciation of the TPM and RGM in the atmosphere due to considerable advances in analytical techniques for RGM and TPM components (Lindberg and Stratton, 1998; Ebinghaus and Kock, 2002; Munthe et al., 2003; Poissant et al., 2005; Gabriel et al., 2005; Lynam and Keeler, 2005; Yatavelli et al., 2006). However, to the authors' knowledge, few field campaigns to determine the distribution of these atmospheric Hg species in ambient air have been conducted in China. Limited studies conducted in urban areas in China have shown that TPM and RGM concentrations in ambient air were highly elevated compared to those observed in Europe and Northern America (Wang et al., 2006; Fang et al., 2001; Xiu et al., 2005; Feng et al., 2002). Due to rapid economic development, China is regarded as the largest Hg emission source in the world (Streets et al., 2005; Wu et al., 2006). Southwestern China is the largest Hg emission region in China, and the annual Hg emission from human activities in Guizhou, Sichuan and Yunan provinces has reached 128 tons (Wu et al., 2006). High concentrations of TGM in the ambient air have been observed in Guiyang city, which were attributed to coal burning in industry and domestic heating (Feng et al., 2004a). Smelting of non-ferrous metals (e.g., Zn) is one of several other important Hg emission sources (Feng et al., 2004b, 2005). In this paper, for the first time the

results of a comprehensive measurement for TPM and RGM in ambient air on the eastern slope of Mt. Gongga, Sichuan province, Southwestern China, are presented and the distribution patterns of these two Hg species in the ambient air in a remote area of China are discussed.

2. Materials and methods

2.1. Study area

Mt. Gongga (29°20′–30°20′ N, 101°30′–102°15′ E) is situated on the Quaternary section of the eastern Qinghai–Tibet Plateau and its transition zone to Sichuan Province. It is the highest mountain in Sichuan province with an elevation of 7556 m above the sea level. Measurements of TGM, TPM and RGM concentrations in the ambient air were performed at the alpine ecosystem observation and experiment station (1640 m elevation) which is located in the NW of Moxi town. This site is regarded as one of the background monitoring stations for air pollutants operated by the Chinese Academy of Sciences (CAS) (Fig. 1). The station is equipped with standard meteorological instruments for temperature, relative humidity, wind direction, wind speed and solar radiation measurements.

Moxi town is situated 200 km SW of Chengdu and 42 km south of Kangding city. The population of Moxi town is about 7000, and the annual coal consumption is about 900 tons. A village with a population of 2000 is located 5 km north of the sampling site. Neighboring industrial areas are situated in two large counties, Shimian and Hanyuan Counties, which are located at 50–60 km south and SE of the sampling site, respectively. The total populations of Shimian and Hanyuan Counties are 120,000 and 340,000, respectively. Non-ferrous metal, especially Zn smelting activities may be an important Hg emission source to the air and the annual production of Zn in Shimian County is more than 10,000 tons. Because of the barrier effect of Mt. Gongga, no seasonal ground wind fields exist in the study area. The wind system near the surface is mainly dominated by the valley wind system regardless of season. In the daytime, air masses are mainly from the SE and Hg-polluted air from Shimian and Hanyuan Counties may be transported to the sampling site; while during the night time, wind from the northwestern mountain side is dominant.

2.2. Experimental

2.2.1. Sampling methods of TPM, RGM and TGM

TPM samples were collected on 6 mm diameter quartz fiber filters (0.45 μm) housed in quartz glass tubes at a nominal flow rate of 2 L min^{-1} (Lu et al., 1998). The quartz fiber filter is cut from a larger quartz fiber filter (47 mm diameter, Millipore) and used only for one sampling and analysis cycle. Two types of denuders (tubular and annular denuders) have been used to sample RGM (Xiao et al., 1997; Feng et al., 2000; Landis et al., 2002), and both of them are coated with KCl film, which has a high adsorption efficiency for RGM while the air is passing through the KCl coated surfaces. TGM in ambient air was sampled using an automated Hg vapor analyzer (Tekran 2537A).

2.2.2. Analysis

Analysis procedures for TPM and RGM described by Lu et al. (1998), Feng et al. (2000)

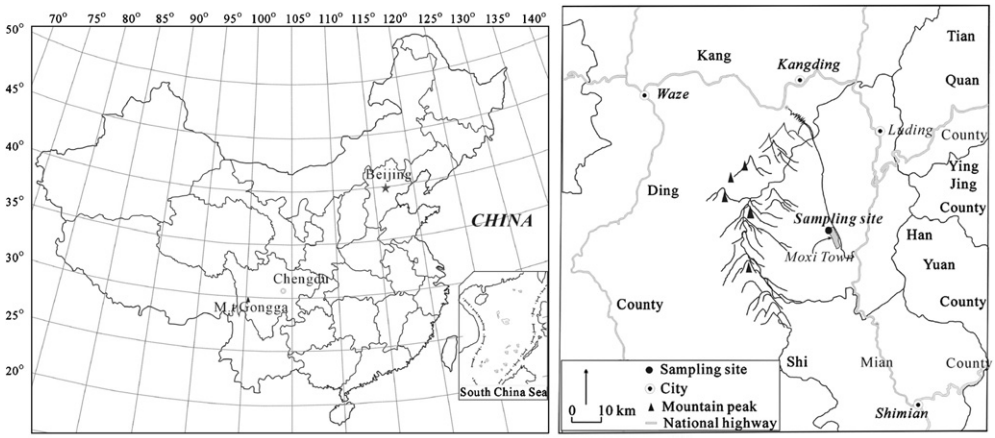

Fig. 1. Location of sampling site on the eastern slope of Mt. Gongga, Sichuan, China.

and Landis et al. (2002) were followed. After sampling, Hg contents are determined via pyrolysis without transfer and handling. The analysis procedure for TPM and RGM consists of three steps and commonly takes 30 min. In the first step, A Tekran 2537A instrument pulls Hg-free air (0.5 L min^{-1}) through the trap and denuders for two sample cycles (10 min), to quantify the zero or background level to ensure no leaks in the system. Then the trap and denuders are rapidly heated to 900 °C and 500 °C for three sample cycles (15 min) for TPM and RGM, respectively. The pyrolyzer converts all Hg compounds to the elemental form and the Hg^0 is subsequently detected by the Tekran 2537A analyzer. Typically, a signal of less than 2 pg is observed in the third heat cycle and this it considered to be the system blank value. The TPM traps and denuders are then cooled by using a cooling fan in the third step.

2.2.3. Sampling of TPM, RGM and TGM

Four sampling campaigns were carried out for TPM and RGM measurements, namely from 25 May to 10 June, 2005, from 15 to 30 September, 2005, 18 December, 2005 to 4 January, 2006 and 18 to 29 April, 2006, representing summer, autumn, winter and spring seasons, respectively. Before sampling, the TPM trap and denuders were pre-cleaned by pyrolysis to obtain operational blanks. TPM traps and denuders were positioned vertically, and the inlets were located at 1.5 m above the ground. During sampling, denuders were heated by heating tapes to a temperature of 20–30 °C above the ambient air temperature in order to prevent condensation of water vapor on the inner surface of the denuder (Feng et al., 2000). The flow rates were controlled by mass-flow controllers (MFC, MKS, USA) which have been calibrated to standard atmospheric pressure (standard temperature of 0 °C and standard pressure of 1013 mbar). The flow rates were 2, 0.75 and 10 L min^{-1} for the TPM trap, tubular denuder and annular denuder, respectively. Sampling time for the TPM trap and tubular denuder was about 22 h (collected air volume: 2.7 m^3 for TPM trap, 1 m^3 for tubular denuder), while sampling time for the annular denuder was 1.5 h (0.9 m^3 air is collected). The time schedules of the campaigns are given in Table 1; during the four campaigns, TPM and RGM (using the tubular denuder method) samples were collected each day starting at 19:00 (local time) and ending at 18:00 the following day. During the sampling periods, TGM concentrations were monitored continuously using a Tekran 2537A with a sampling time of 5 min. TGM concentrations were averaged for the RGM and TPM sampling periods.

Table 1
The time schedules of the measurement campaigns

Sampling method	Campaign	Start date	Stop date
TPM trap and tubular denuder	Summer	May 25, 2005	Jun 10, 2005
	Autumn	September 15, 2005	September 30, 2005
	Winter	December 18, 2005	January 4, 2006
	Spring	April 18, 2006	April 29, 2006
Annular denuder	Winter	December 19, 2005	December 28, 2005

2.2.4. Wet deposition

Precipitation samples were collected by using a bulk sampler with an acid-washed borosilicate glass bottle and a borosilicate glass wide-mouthed (15 cm diameter) jars supported in a PVC housing system (Oslo and Paris Commission, 1998). For the days with no precipitation, the wide-mouthed jar was sealed to protect particulate matter from depositing on the open collector, and the collector was set out just prior to or within 15 min of the beginning of a precipitation event. However, this method inevitably resulted in loss of some precipitation samples because some rain events occurred at night. The collection efficiency of the sampling method was calculated to be 81.9% from a comparison between precipitation collected and measured from the meteorological station. Precipitation samples were preserved with 5 mL L^{-1} HCl (Suprapur) and stored in a Teflon bottle (250 mL) at 4 °C in the refrigerator. After completion of the measurement campaigns, the precipitation samples were rapidly brought to the laboratory for analysis. Total Hg concentrations in precipitation samples were determined by a standard method, i.e., BrCl oxidation, Sn(II) reduction and pre-concentration via Au-amalgamation followed by CVAAS detection (US EPA, 1999).

3. Results and discussion

3.1. Reproducibility test

Fig. 2 shows the reproducibility test results of TPM and RGM in ambient air. For TPM, the

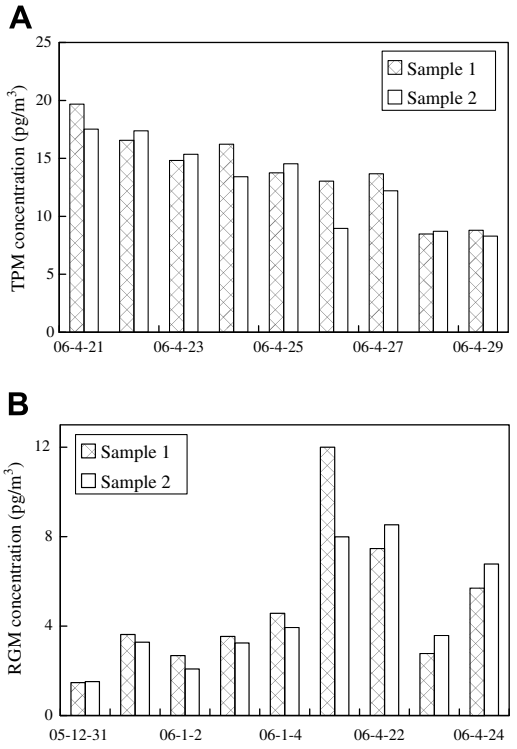

Fig. 2. The reproducibility test results of TPM and RGM sampling methods: (A) TPM and (B) RGM.

reproducibility test was carried out in April 2006 (Fig. 2A), and nine pairs of parallel sampling tests were performed. Although the standard deviation of one sample pair performed on 26 April, 2006 was as large as 31%, the overall reproducibility was 10%. RGM reproducibility tests were performed in two sampling campaigns (Fig. 2B); five sample pairs were taken from 31 December to 4 January, 2006, while the other four were monitored in April 2006. During the two RGM parallel sampling periods, the overall reproducibility is 16% (ranging from 3% to 33%). The tests demonstrated that the sampling methods can reproducibly collect both RGM and TPM.

3.2. Concentrations of TPM, RGM and TGM

Statistical summaries of TPM, RGM and TGM concentrations measured in this remote area of Southwestern China are shown in Table 2. The average concentrations of TPM, RGM and TGM were 30.7 pg m^{-3}, 6.2 pg m^{-3} and 4.7 ng m^{-3}, respectively. Strong temporal variability of TPM and RGM concentrations were observed as shown in Fig. 3, and the daily concentrations of TPM and RGM ranged from 5.2 to 135.7 and 1.5 to 22.5 pg m^{-3}, respectively. TPM and RGM concentrations were both characterized by low variability during the spring sampling campaign, however, higher variability was observed in the other three campaigns. The largest variability of TPM concentrations was observed in autumn, while the highest variability of RGM concentrations was observed in summer with the greatest variability of solar time and more precipitation events (Table 2).

It is generally accepted that TPM measured without a denuder installed upstream can be overestimated because of adsorption of RGM, and Lynam and Keeler (2002) suggested that the magnitude of the artifact is probably related to concentration of RGM. Unfortunately, TPM was not collected downstream of RGM because different flow rates were selected for sampling of TPM (2 L min^{-1}) and RGM (0.75 L min^{-1}). However, the authors consider that artifact TPM should be very low because the RGM concentration was extremely low in this case. In research on the distribution of TPM in Northern Europe, Wängberg et al. (2003) found that fairly low RGM concentrations (<15 pg m^{-3}) did not cause overestimation of TPM and the artifact was not observed even when RGM concentration was elevated (>40 pg m^{-3}). Fig. 4 shows the time series of TPM and RGM in the April 2006 campaign during which the highest mean seasonal RGM concentration was observed; it is clear that RGM is not correlated with TPM ($R = 0.12$, $P = 0.71$), indicating no artifacts of TPM from RGM results from this study site.

Except during winter, TPM and RGM in the Mt. Gongga area showed background levels characteristic of these Hg species in China, and they are more than an order of magnitude lower than those measured in some urban areas in China (Fang et al., 2001; Zheng et al., 2005; Xiu et al., 2005; Wang et al., 2006). The results are comparable to the statistical mean TPM and RGM from global rural/remote sites (mean: 18 pg m^{-3} (RGM); 21 pg m^{-3} ($PM_{2.5}$), Valente et al., 2007).

The study found that the mean concentration of TPM was higher than that of RGM during the four sampling campaigns, which is consistent with those observations conducted in some remote areas in Canada (Poissant et al., 2004, 2005; Zhang et al., 2005). On average, the measured TPM to RGM ratio was 5, which was slightly higher than that obtained from the Bay St. Francois wetland,

Table 2
A statistical summary for the concentrations of total particulate mercury (TPM), reactive gaseous mercury (RGM), total gaseous mercury (TGM) and the meteorological parameters measured during the four sampling campaigns

	TPM (pg m^{-3})	RGM (pg^{-3})	TGM (ng m^{-3})	Solar time (h)	Temperature (°C)	Rainfall (mm)	Humidity (%)	Wind speed (s/m)
May 25–June 10, 2005								
Average	10.8	5.9	3.3	2.9	18.0	5.1	79.4	1.0
Median	9.9	4.7	3.3	2.0	18.2	2.7	80.8	1.0
Maximum	21.8	22.5	4.5	9.2	20.5	15.8	90.1	1.7
Minimum	5.2	1.5	2.0	0	15.9	0	58.2	0.6
Variation coefficient (CV)	0.42	0.89	0.2	1.06	0.07	1.10	0.11	0.28
N	16	16	16	16	16	16	16	16
September 15–September 30, 2005								
Average	22.5	7.0	4.8	2.9	18.7	1.8	81.8	0.5
Median	21.4	5.2	4.7	2.1	18.2	0.6	81.9	0.4
Maximum	51.3	17.0	8.8	6.8	22.0	7.5	88.8	0.9
Minimum	5.2	3.0	2.1	0	16.4	0	73.4	0.2
Variation coefficient (CV)	0.59	0.59	0.4	1.19	0.10	1.19	0.05	0.43
N	15	15	15	15	15	15	15	15
December 18, 2005–January 4, 2006								
Average	74.1	4.0	7.1	3.8	4.8	0	70.6	0.9
Median	68.0	4.1	7.1	4.3	5.1	0	70.5	0.8
Maximum	135.7	7.5	10.4	7	7.1	0	81.5	1.2
Minimum	39.0	1.5	4.5	0	2.4	0	63.9	0.6
Variation coefficient (CV)	0.4	0.4	0.2	0.66	0.32	-	0.07	0.24
N	17	17	17	17	17	17	17	17
April 18, 2006–April 29, 2006								
Average	15.3	8.0	3.7	5.5	16.3	2.4	65.5	1.25
Median	15.0	7.1	3.7	5.4	16.5	0.4	64.3	1.25
Maximum	21.6	13.5	5.4	10.2	17.4	12.2	76.5	2.0
Minimum	8.5	3.2	2.0	0	14.8	0	50.0	0.7
Variation coefficient (CV)	0.29	0.33	0.2	0.58	0.05	1.63	0.14	0.30
N	12	12	12	12	12	12	12	12
Total average	30.7	6.2	4.7	3.8	14.5	2.3	74.4	0.9

Québec, Canada (ratio: 3, Poissant et al., 2004), but lower than that measured in the St. Anicet area, Québec, Canada (ratio: 8, Poissant et al., 2005). This might indicate that RGM has a lower atmospheric residence time and is more likely than TPM to be scavenged (Poissant et al., 2004; Zhang et al., 2005).

Generally, municipal waste incinerators and coal-fired power plants are the sources of TPM and RGM in the ambient air (Prestbo and Bloom, 1995). High concentrations of TPM and RGM observed in urban areas of China might suggest high emissions of both TPM and RGM in these areas and also reflect the difference in coal consumption and control technologies between China and Northern Europe and North America (Xiu et al., 2005). Some studies have depicted the distributions of TPM and RGM concentrations worldwide by using a multiscale modeling system (Seigneur et al., 2004; Shia et al., 1999). These modeling studies predict that TPM and RGM concentrations in Southwestern China are in the range of 75–100 pg m^{-3}. It can be seen from the present data that RGM concentration, in particular, and TPM is much lower than the modeling results except for TPM concentration observed during winter. It is generally accepted that TPM and RGM have shorter atmospheric residence times than TGM and their transport scale is relatively restricted (Lindberg and Stratton, 1998; Poissant et al., 2004; Landis et al., 2004). Lower TPM and RGM concentration in the study area compared to the

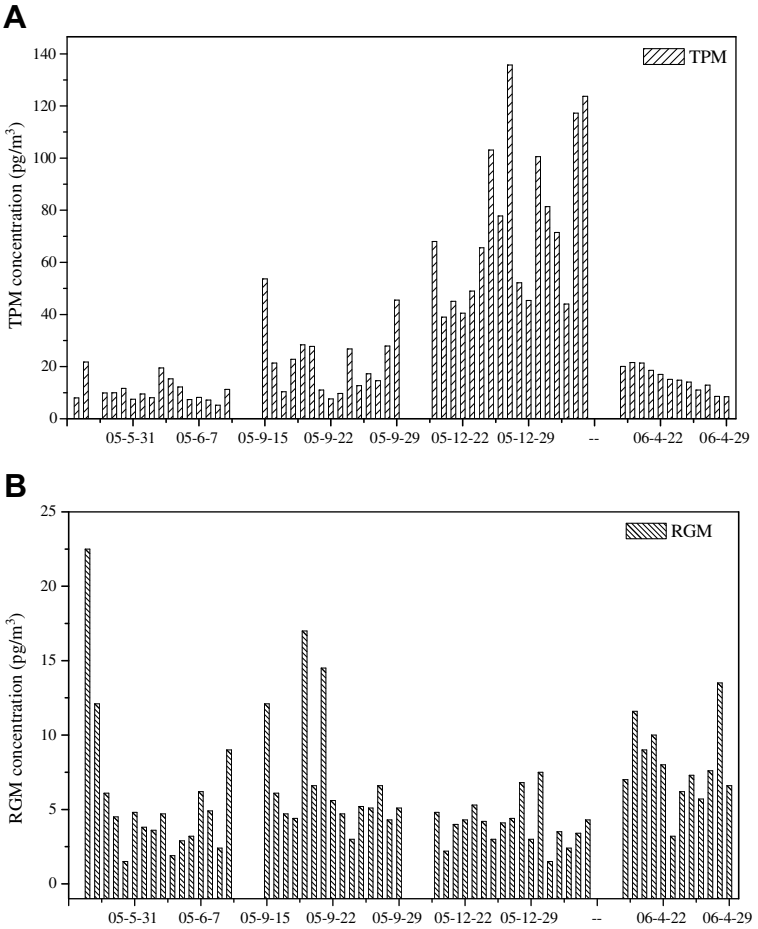

Fig. 3. Time series plots of (A) total particulate mercury (TPM) concentrations and (B) reactive gaseous mercury (RGM) concentrations.

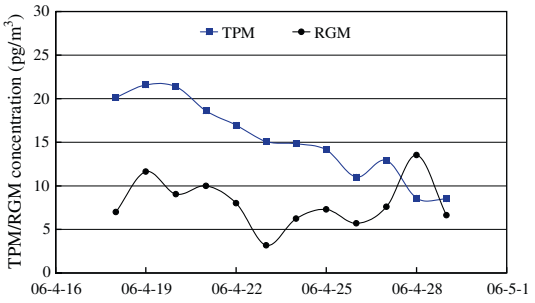

Fig. 4. Time series concentrations of TPM and RGM during the sampling campaign conducted in April 2006.

modeling results might suggest that distribution of TPM and RGM has much variability and more field measurements are needed. Fu et al. (2007) found that Hg emission from Shimian and Hanyuan County contributed significantly to the highly elevated TGM concentration at the Moxi sampling site. Fig. 5 shows RGM and TPM concentrations plotted vs. TGM. It is clear that TPM is significantly correlated with TGM concentrations whereas no significant correlation was observed between RGM and TGM concentrations. This may suggest that TPM and TGM at the Moxi sampling site shared a similar pollution source – the Shimian and Hanyuan industrial area. However, because of the extremely high dry deposition velocity of RGM, emission of Hg from the industrial area had less effect on RGM at the sampling site. This is quite consistent with previous studies showing that TPM can travel a long distance whereas RGM transport is highly restricted (Wängberg et al., 2003; Wang et al., 2006; Landis et al., 2004).

Fig. 6 depicts the median seasonal concentrations of TPM and RGM on the eastern slope of the Mt. Gongga area. A remarkable seasonal distribution

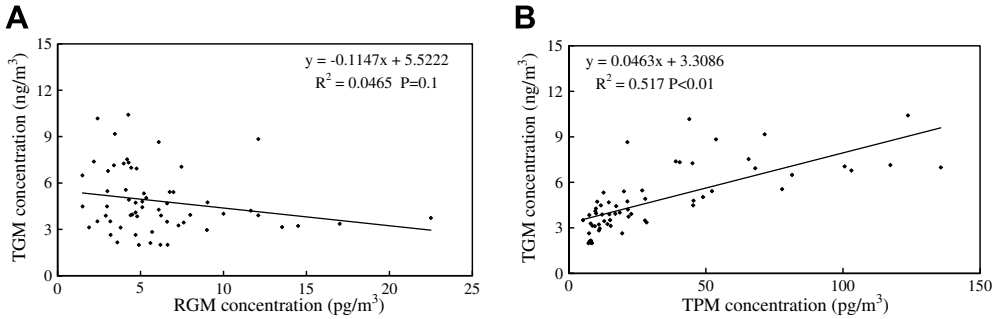

Fig. 5. Correlation analysis between the daily mean concentrations of (A) RGM and TGM and (B) TPM and TGM.

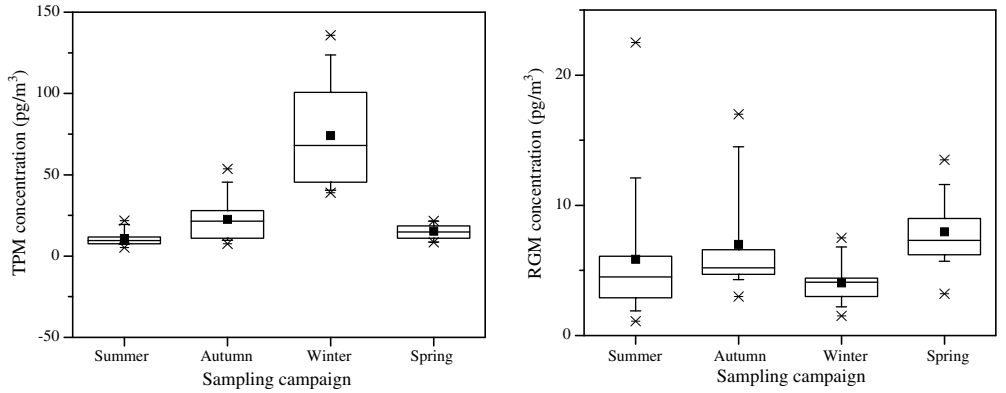

Fig. 6. Seasonal variations of TPM and RGM concentrations. Seasonally mean concentrations are indicated by solid square. The lower boundary of the box indicates the 25th percentile, a line within the box marks the median, while the upper boundary of the box indicates the 75th percentile. Whiskers indicate the 1st, 10th, 90th and 99th percentiles.

pattern of TPM concentrations and a slight seasonal change of RGM concentrations were observed (Fig. 6). TPM showed a maximum mean concentration in the winter sampling campaign and a minimum mean concentration in the summer campaign, and the mean TPM concentration in winter was 6.9 times higher than that in summer, while RGM concentrations were slightly higher in spring and autumn than in other seasons. Similar seasonal distribution of TPM and RGM concentrations was also observed in Athens, OH, USA (Yatavelli et al., 2006). Seasonal variations of TPM concentrations are well documented in previous studies (Wang et al., 2006; Zielonka et al., 2005) which have demonstrated that enhanced regional coal burning and low wet deposition velocity in winter might contribute to the elevated TPM concentrations. Unlike the TPM concentration controlled by both regional and local emissions, RGM is controlled mostly by local emissions. There are no pollution control devices used during domestic coal burning in the local areas so that more airborne particulate matter will be released to the air, which will absorb RGM to form particulate Hg. Therefore, the emission factors of RGM from domestic coal burning could be very low (Feng, 1997). Besides, some studies also suggest that stronger partitioning of gaseous Hg to the particulate phase would decrease RGM concentration especially in winter with lower ambient temperature (Poissant et al., 2005; Lynam and Keeler, 2005). Thus, enhanced coal use in winter for home heating in Moxi town did not increase the RGM concentrations in the ambient air of the sampling site.

Fig. 7 shows the RGM concentrations obtained in December, 2005 using annular denuders. These values were in good agreement with the daily concentration observed using tubular denuders and suggested that both methods were comparable. A clear diurnal RGM distribution pattern obviously related to ultraviolet radiation was observed during the sampling campaign as shown in Fig. 7. Similar diurnal cycles have also been observed in previous

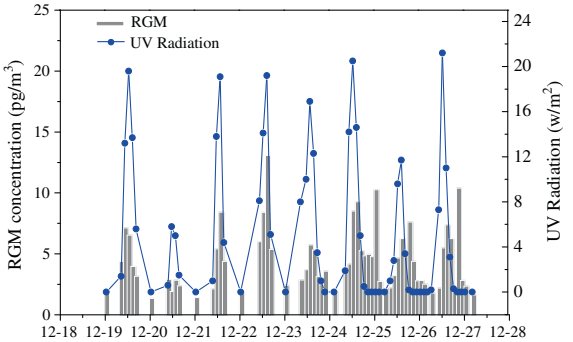

Fig. 7. Diurnal pattern of RGM concentration and ultraviolet radiation in December, 2006.

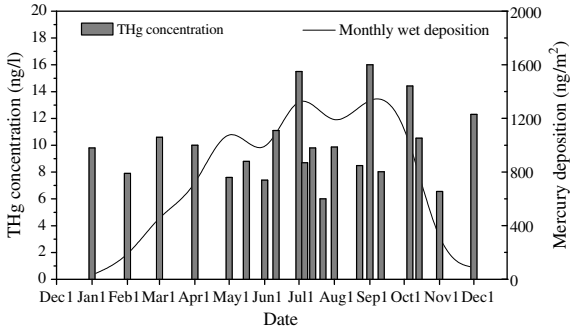

Fig. 8. Time series sets of THg concentrations in precipitation and deposition flux at Moxi sampling site, measured from 1 January, to 31 December, 2006.

studies (Lindberg and Stratton, 1998; Lynam and Keeler, 2005; Poissant et al., 2005; Yatavelli et al., 2006), and these studies also suggested that this diurnal cycle might be influenced by photo-oxidation processes and sharp depletion building up under the stable boundary layer during the night. However, the transformation of Hg^0 to the RGM form is not well understood. Some studies have suggested that reaction may occur between Hg^0 and atmospheric oxidants (e.g., O_3 and OH), but according to recent findings this process is probably not occurring or is too slow to be important in the production of RGM in the daytime (Calvert and Lindberg, 2005; Bauer et al., 2003; Goodsite et al., 2004). Thus, more field and laboratory studies are needed to focus on the reaction mechanism between Hg^0 and atmospheric oxidants.

3.3. Wet deposition

Total Hg concentrations in precipitation samples collected from January to December, 2006 ranged from 6.0 to 16.0 ng L^{-1} (Fig. 8), and the volume-weighted mean concentration was 9.9 ± 2.8 ng L^{-1}, using volume results from the meteorological station. There was no obvious seasonal variation of THg concentrations in rain samples. However, three precipitation samples whose THg concentrations exceeding 14 ng L^{-1} were observed in the rainy season. It is well established that precipitation rate, rain type, characteristics of pollutants, gaseous and aqueous Hg chemistry might play important roles in determining the distribution of Hg in rain samples (Abbott et al., 2002; Lin et al., 2006). The highest THg concentration (16.0 ng L^{-1}) observed on 1 September and 10 September was associated with the highest precipitation rate (72.7 mm), and this may suggest a higher scavenging coefficient caused by higher precipitation rate.

The annual wet deposition flux (9.1 μg m^{-2}) was calculated using the annual value-weighted mean THg concentration and total precipitation. This value is similar to those measured at the Experimental Lakes Area in Northwestern Ontario, Canada and a rural super-site in Athens, OH, USA (St. Louis et al., 2001; Yatavelli et al., 2006). Since the THg concentrations in precipitation did not change seasonally, the seasonal changes of precipitation rates contributed much to the seasonal distribution of wet deposition flux of Hg. The total Hg wet deposition flux was 7.3 μg m^{-2} in rainy seasons (May, 2006–October, 2006) which accounted for 80% of total annual wet deposition. The efficient wet scavenging process in the rainy season might be an important reason for the low TPM concentration in this period.

4. Summary and conclusions

Measurements of TPM and RGM in ambient air were carried out on the eastern slope of Mt. Gongga, at the Southeastern margin of the Tibetan plateau. Average TPM and RGM concentrations in the study site are 30.7 and 6.2 pg m^{-3}, which are comparable to mean TPM and RGM concentrations from global rural/remote sites, but much lower than those observed in some urban areas in China. A distinctly seasonal distribution pattern of TPM was observed during the measurement period with TPM concentrations listed in descending order: winter (74.1 pg m^{-3}), autumn (22.5 pg m^{-3}), spring (15.3 pg m^{-3}) and summer (10.8 pg m^{-3}). Compared to other seasons, a slightly higher con-

centration of RGM was observed in spring (8.0 pg m^{-3}) and the minimum concentration of RGM was observed in winter (4.0 pg m^{-3}) in which TPM concentration was highly elevated. Different seasonal distribution pattern for TPM and RGM might be attributed to the sources and physical/chemical properties of these two Hg species in the air. Increased coal use and special weather conditions in winter might contribute to the elevated TPM concentrations; while the seasonal and daily cycles of RGM concentrations might indicate that some transformations between Hg^0 and RGM were involved. The volume-weighted mean concentration of THg was 9.9 ng L^{-1} and the total annual wet deposition flux was 9.1 μg m^{-2}. No seasonal variation of THg concentrations in precipitation was observed and intensity of rainfall determined that the primary wet deposition of Hg occurred in the rainy season.

Acknowledgements

This research was financially supported by the Chinese Academy of Sciences through an Innovation Foundation Award (KZCX3-SW-443), with additional support from the Field Station Foundation, the International Partnership Project and the Natural Science Foundation of China (40532014).

References

Abbott, M.L., Susong, D.D., Krabbenhoft, D.P., Rood, A.S., 2002. Mercury deposition in snow near an industrial emission source in the western US and comparison to ISC3 model predictions. Water Air Soil Pollut. 139, 95–114.

Bauer, D., D'Ottone, L., Campuzaon-Jost, P., Hynes, A.J., 2003. Gas phase elemental mercury: a comparison of LIF detection techniques and study of the kinetics of reaction with the hydroxyl radical. J. Photochem. Photobiol. A 157, 247–256.

Calvert, J.G., Lindberg, S.E., 2005. Mechanisms of mercury removal by O3 and OH in the atmosphere. Atmos. Environ. 39, 3355–3367.

Ebinghaus, R., Kock, H.H., 2002. Antarctic springtime depletion of atmospheric mercury. Environ. Sci. Technol. 36, 1238–1244.

Fang, F., Wang, Q., Li, J., 2001. Atmospheric particulate mercury in Changchun City, China. Atmos. Environ. 35, 4265–4272.

Feng, X.B., 1997. Development of analytical methods for determination of trace mercury in environmental samples and the modes of occurrence of mercury in coal from coal in Guizhou. PhD Dissertation. Institute of Geochemistry, Chinese Academy of Sciences.

Feng, X.B., Li, G.H., Qiu, G.L., 2004b. A preliminary study on mercury contamination to the environment from artisanal zinc smelting using indigenous methods in Hezhang County, Guizhou, China—Part 1: mercury emission from zinc smelting and its influences on the surface waters. Atmos. Environ. 38, 6223–6230.

Feng, X.B., Li, G.H., Qiu, G.L., 2005. A preliminary study on mercury contamination to the environment from artisanal zinc smelting using indigenous methods in Hezhang County, Guizhou, China: Part 2 Mercury contaminations to soil and crop. Sci. Total Environ. 368, 47–55.

Feng, X.B., Sommar, J., Gardfeldt, K., Lindqvist, O., 2000. Improved determination of gaseous divalent mercury in ambient air using KCl coated denuders. Fres. J. Anal. Chem. 366, 423–428.

Feng, X.B., Sommar, J., Lindqvist, O., Hong, Y., 2002. Occurrence, emissions and deposition of mercury during coal combustion in the province Guizhou, China. Water Air Soil Pollut. 139, 311–324.

Feng, X.B., Tang, S.L., Shang, L.H., Yan, H.Y., Zheng, W., 2004a. Temporal variation of total gaseous mercury in the air of Guiyang, China. J. Geophys. Res. 109, D03303, 1.

Fitzgerald, W.F., 1995. Is mercury increasing in the atmosphere? The need for an atmospheric mercury network (AMNET). Water Air Soil Pollut. 80, 245–254.

Fu, X.W., Feng, X.B., Zhu, W.Z., 2007. Total gaseous mercury concentrations in ambient air in the eastern slope of Mt. Gongga, South-Eastern fringe of the Tibetan plateau, China. Atmos. Environ., doi:10.1016/j.atmosenv.2007.10.018.

Gabriel, M., Williamsona, D.G., Brooksb, S., Lindberg, S.E., 2005. Atmospheric speciation of mercury in two contrasting Southeastern US airsheds. Atmos. Environ. 39, 4947–4958.

Goodsite, M.E., Plane, J.M.C., Skov, H., 2004. A theoretical study of the oxidation of Hg^0 to $HgBr_2$ in the troposphere. Environ. Sci. Technol. 38, 1772–1776.

Landis, M.S., Keelerb, G.J., Al-Walib, K.I., Stevensc, R.K., 2004. Divalent inorganic reactive gaseous mercury emissions from a mercury cell chlor-alkali plant and its impact on near-field atmospheric dry deposition. Atmos. Environ. 38, 613–622.

Landis, M.S., Stevens, R.K., Schaedlich, F., Prestbo, E.M., 2002. Development and characterization of an annular denuder methodology for the measurement of divalent inorganic reactive gaseous mercury in ambient air. Environ. Sci. Technol. 36, 3000–3009.

Lee, D.S., Nemitz, E., Fowler, D., Kingdon, R.D., 2001. Modeling atmospheric mercury transport and deposition across Europe and the UK. Atmos. Environ. 35, 5455–5466.

Lin, C.J., Pongprueksa, P., Lindberg, S.E., Pehkonen, S.O., Byun, D., Jang, C., 2006. Scientific uncertainties in atmospheric mercury models: model science evaluation. Atmos. Environ. 40, 2911–2928.

Lindberg, S.E., Stratton, W.J., 1998. Atmospheric speciation concentrations and behavior of reactive gaseous mercury in ambient air. Environ. Sci. Technol. 32, 49–57.

Lindberg, S.E., Landis, M.S., Stevens, R.K., Brooks, S., 2001. Comments on atmospheric mercury species in the European Arctic: measurements and modeling by Berg et al. Atmos. Environ. 35, 5377–5378.

Lorey, P., Driscoll, C.T., 1999. Historical trends of mercury deposition in Adirondack lakes. Environ. Sci. Technol. 33, 718–722.

Lu, J.Y., Schroeder, W.H., 2004. Annual time-series of total filterable atmospheric mercury concentrations in the Arctic. Tellus B 56, 213–222.

Lu, J.Y., Schroeder, W.H., Berg, T., Munthe, J., Schneeberger, D., Schaedlich, F.A., 1998. Device for sampling and determination of total particulate mercury in ambient air. Anal. Chem. 70, 2403–2408.

Lynam, M.M., Keeler, G.J., 2002. Comparison of methods for particulate phase mercury analysis: sampling and analysis. Anal. Bioanal. Chem. 374, 1009–1014.

Lynam, M.M., Keeler, G.J., 2005. Automated speciated mercury measurements in Michigan. Environ. Sci. Technol. 39, 9253–9262.

Miller, E.K., Vanarsdale, A., Keeler, G.J., Chalmers, A., Poissant, L., Kamman, N.C., Brulotte, R., 2005. Estimation and mapping of wet and dry mercury deposition across Northeastern North America. Ecotoxicology 14, 53–70.

Munthe, J., Wängberg, I., Iverfeldt, Å., Lindqvist, O., 2003. Distribution of atmospheric mercury species in Northern Europe: final results from the MOE project. Atmos. Environ. 37, 9–20.

Oslo and Paris Commission, 1998. JAMP guidelines for the sampling and analysis of mercury in air and precipitation. Joint Assessment and Monitoring Programme, pp. 1–20.

Pacyna, J.M., Pacyna, E.G., Streenhuisen, F., Wilson, S., 2003. Mapping 1995 global anthropogenic emission of mercury. Atmos. Environ. 37, 109–117.

Poissant, L., Pilote, M., Beauvais, C., Constant, P., Zhang, H.H., 2005. A year of continuous measurements of three atmospheric mercury species (GEM, RGM and Hg–P) in southern Québec, Canada. Atmos. Environ. 39, 1275–1287.

Poissant, L., Pilote, M., Xu, X., Zhang, H., Beauvais, C., 2004. Atmospheric mercury speciation and deposition in the Bay St. Francois wetlands. J. Geophys. Res. 109, D11301.

Prestbo, E.M., Bloom, N.S., 1995. Mercury speciation adsorption (MESA) method for combustion flue gas: methodology, artifacts, intercomparison and atmospheric implications. Water Air Soil Pollut. 80, 145–158.

Schroeder, W.H., Munthe, J., 1998. Atmospheric mercury—an overview. Atmos. Environ. 32, 809–822.

Schuster, P.F., Krabbenhoft, P.F., Naftz, D.L., Cecil, L.D., Olson, M.L., Dewild, J.F., Susong, D.D., Green, J.R., Abbott, M.L., 2002. Atmospheric mercury deposition during the last 270 years: a glacial ice core record of natural and anthropogenic sources. Environ. Sci. Technol. 36, 2303–2310.

Seigneur, C., Lohman, K., Vijayaraghavan, K., Shia, R.L., 2003. Contributions of global and regional sources to mercury deposition in New York state. Environ. Pollut. 123, 365–373.

Seigneur, C., Vijayaraghavan, K., Lohman, K., Karamchandani, P., Scott, C., 2004. Global source attribution for mercury deposition in the United States. Environ. Sci. Technol. 38, 555–569.

Shia, R.-L., Seigneur, C., Pai, P., Ko, M., Sze, N.D., 1999. Global simulation of atmospheric mercury concentrations and deposition fluxes. J. Geophys. Res. 4, 23747–23760.

Louis, V.L., Rudd, J.W.M., Kelly, C.A., Hall, B.D., Rolfhus, K.R., Scott, K.J., Lindberg, S.E., Dong, W.J., 2001. Importance of the forest canopy to flux of methylmercury and total mercury to boreal ecosystems. Environ. Sci. Technol. 35, 3089–3098.

Streets, D.G., Hao, J.M., Jiang, J.K., Chan, M., Tian, H.Z., Feng, X.B., 2005. Anthropogenic mercury emissions in China. Atmos. Environ. 39, 7789–7806.

Tan, H., He, J.L., Liang, L., Lazoff, S., Sommer, J., Xiao, Z.F., Lindqvist, O., 2000. Atmospheric mercury deposition in Guizhou, China. Sci. Total Environ. 259, 223–230.

US EPA, 1999. Method 1631, Revision B: Mercury in water by Oxidation, Purge and Trap, and Cold Vapor Atomic Fluorescence Spectrometry. US Environmental Protection Agency, pp. 1–33.

Valente, R.J., Shea, C., Humes, K.L., Tanner, R.L., 2007. Atmospheric mercury in the Great Smoky Mountains compared to regional and global levels. Atmos. Environ. 41, 1861–1873.

Wang, Z., Zhang, X., Chen, Z., Zhang, Y., 2006. Mercury concentrations in size-fractionated airborne particles at urban and suburban sites in Beijing, China. Atmos. Environ. 40, 2194–2201.

Wängberg, I., Munthe, J., Ebinghaus, R., Gårdfeldt, K., Iverfeldt, Å., Sommar, J., 2003. Distribution of TPM in Northern Europe. Sci. Total Environ. 304, 53–59.

Wu, Y., Wang, S.X., Streets, D.G., Hao, J.M., Chan, M., Jiang, J.K., 2006. Trends in anthropogenic mercury emissions in China from 1995 to 2003. Environ. Sci. Technol. 40, 5312–5318.

Xiu, G., Jin, Q., Zhang, D., Shi, S., 2005. Characterization of size-fractionated particulate mercury in Shanghai ambient air. Atmos. Environ. 39, 419–427.

Xiao, Z., Sommar, J., Wei, S., Lindqvist, O., 1997. Sampling and determination of gas phase divalent mercury in the air using a KCl coated denuder. Fres. J. Anal. Chem. 358, 386–391.

Yang, H.D., Rose, N.L., 2003. Distribution of mercury in six lake sediment cores across the UK. Sci. Total Environ. 304, 391–404.

Yatavelli, R.L.N., Fahrnia, J.K., Kim, M., Crist, K.C., Vickers, C.D., Winter, S.E., Connell, D.P., 2006. Mercury, $PM_{2.5}$ and gaseous co-pollutants in the Ohio River Valley region: preliminary results from the Athens supersite. Atmos. Environ. 40, 6650–6665.

Zhang, H.H., Poissant, L., Xu, X.H., Pilote, M., 2005. Explorative and innovative dynamic flux bag method development and testing for mercury air–vegetation gas exchange fluxes. Atmos. Environ. 39, 7481–7493.

Zhang, L., Gong, S., Padro, J., Barrie, L., 2001. A size-segregated particle dry deposition scheme for an atmospheric aerosol module. Atmos. Environ. 35, 549–560.

Zheng, W., Feng, X., Li, Z.G., 2005. Determination of total particulate mercury in atmosphere. Bull. Mineral Petrol. Geochem. 24, 333–336 (in Chinese).

Zielonka, U., Hlawiczka, S., Fudala, J., Wängberg, I., Munthe, J., 2005. Seasonal mercury concentrations measured in rural air in Southern Poland contribution from local and regional coal combustion. Atmos. Environ. 39, 7580–7586.